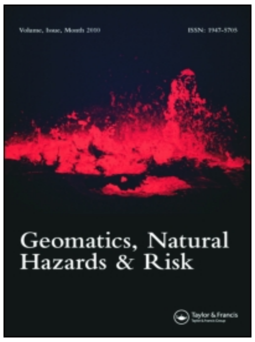

Geomatics, Natural Hazards and Risk

ISSN: 1947-5705 (Print) 1947-5713 (Online) Journal homepage: http://www.tandfonline.com/loi/tgnh20

Rainstorm-induced shallow landslides process and evaluation – a case study from three hot spots, China

Weiyue Li, Chun Liu, Yang Hong, Manabendra Saharia, Weiwei Sun, Dongjing Yao & Wen Chen

GEOMATICS, NATURAL HAZARDS AND RISK, 2016
VOL. 7, NO. 6, 1908–1918
http://dx.doi.org/10.1080/19475705.2016.1179685

Taylor & Francis
Taylor & Francis Group

Rainstorm-induced shallow landslides process and evaluation – a case study from three hot spots, China

Weiyue Li[a], Chun Liu[b], Yang Hong[c,d], Manabendra Saharia[c], Weiwei Sun[e], Dongjing Yao[f] and Wen Chen[g]

[a]Institute of Urban Study, Shanghai Normal University, Shanghai 200234, China; [b]College of Surveying and Geo-Informatics, Tongji University, Shanghai 200029, China; [c]School of Civil Engineering and Environmental Sciences, University of Oklahoma, OK 73072, USA; [d]Department of Hydraulic Engineering, Tsinghua University, Beijing 100084, China; [e]College of Architectural Engineering, Civil Engineering and Environment, Ningbo University, Ningbo 315211, China; [f]Department of Geography, Shanghai Normal University, Shanghai 200234, China; [g]Engineering Center of SHMEC for Space Information and GNSS, East China Normal University, Shanghai 200062, China

ABSTRACT
The critical stage in the evaluation of rainfall-induced landslide failure is in formulating reasonable models to better simulate spatiotemporal changes of slopes in the hilly terrains. A physically based model can take into account the contribution of rainfall infiltration and shear strength of saturated soil layer, and therefore help revealing the landslide formation mechanisms. This paper presents a physically based approach to simulate the landslide process triggered by rainstorm. On the basis of previous solutions, we select the simplified infiltration model Slope-Infiltration-Distributed Equilibrium (SLIDE) to illustrate the dynamical relations between factor of safety (FS) and accumulation of rainfall over time. This model is tested with three representative landslide events in the southwest, southeast, and south central of China during rainstorm. Results show that the time of landslide failure predicted from the SLIDE model is consistent with the reality. Meanwhile, this paper illustrates the differences of FS among the different slope gradients in the vicinity of same soil texture and relationship between FS and rainfall accumulation. This work formulates a methodology of rainstorm-induced landslide evaluation and improves upon the existing landslide prediction methods.

ARTICLE HISTORY
Received 15 July 2015
Accepted 14 April 2016

KEYWORDS
Rainfall-induced landslides; spatiotemporal; SLIDE; FS; rainfall accumulation

1. Introduction

Under the circumstances of global climate changes, overpopulation, deforestation, tectonic stress, etc., landslide has been the most frequent and severe natural hazard (Guzzetti et al. 1999; Heersink 2005). China experiences some of the most serious landslides, and has been trapped with the largest number of fatalities in the world (Petley 2012). Over 90,000 hidden threats from landslide failures occur in the south and northwest of China (Huang & Li 2011). In particular, landslides induced by heavy rainfall are the most frequently described event in news reports. Rainfall, especially heavy rainfall, is a trigger to change the structure of soil and the surrounding conditions of underwater. The lasting heavy rainfall increases soil pore water pressure and decreases soil cohesion in the subsurface, thereby activating the driving forces on the slope (Kirschbaum et al. 2012a).

CONTACT Dongjing Yao dongjingyao2015@126.com

Currently, empirical or statistical techniques are generally utilized for landslide susceptibility analysis studies with some affected factors (lithology, slope gradient, elevation, soil texture, vegetation, land cover, etc.) at all kinds of scales (Hong et al. 2007; Liao et al. 2011). In the susceptibility areas, rainfall-induced landslides can be predicted from the relationship between landslide occurrences and rainfall intensity-duration thresholds (Caine 1980; Hong & Adler 2008). Although the method can identify the location and time of landslide, the accuracy is dependent on the landslide records and some uncertain factors. Study on rainfall-induced landslides has increased the understanding of triggering mechanics which is one of the most important and difficult issues (Kirschbaum et al. 2012b). Some representative physically based models have been developed for landslide evaluation using slope stability calculation (Dietrich & Montgomery 1998; Pack et al. 1998; Iverson 2000; Beek & Asch 2004; Baum et al. 2008). The dynamic models among them include STARWARS+PROBSTAB and TRIGRS to simulate the process of landslide stability (Kuriakose et al. 2008). They are generally process-driven models and employ high-resolution terrain data, soil texture information, rainfall measure at the land surface, and accurate landslide records. Unfortunately, the above models are complicated, and do not work fast evaluation of landslide because of surface heterogeneity and sparse parameters setting. Slope-Infiltration-Distributed Equilibrium (SLIDE), improved from TRIGRS, is a simplified physical model for identifying the spatiotemporal distribution at every landslide grids, representing one-dimensional vertical rainfall infiltration from hours to a few days in the rainstorm (Liao et al. 2012). Particularly, SLIDE can reveal the rainstorm-induced landslide process when the shallow surface of soil reaches saturation and has great potential for rainstorm-induced landslide evaluation.

In this manuscript, we implement the SLIDE model to verify landslide process and evaluation in the rainstorm situation – a case study from three hot spots in China. Moreover, we would like illustrate the relationships between factor of safety (FS) and three slope affected factors (slope angle, time and rainfall accumulation) in the same soil-texture regions.

2. Methodology

2.1. SLIDE model

In the general landslide process, the seepage field of slope changes because of rainfall infiltration, and results in increasing pore-water pressure and seepage force (F) and, meanwhile, decreasing matrix suction and shear force (T). When F is more than T, slope instability may cause landslide (figure 1).

N is the normal effective force; tn is the time step of infiltration; H is the thickness of the potentially unstable layer; H_{sat} is the thickness of the saturated layer; and α is the slope gradient. FS is expressed as the value (T/F) to confirm slope stability. A slope is stable when FS > 1, and unstable when FS ≤ 1.

The SLIDE model was developed based on the TRIGRS model from Hydrometeorology and Remote Sensing Laboratory, the University of Oklahoma (http://hydro.ou.edu/research/model/). It illustrates the impact of heavy rainfall on apparent cohesion to the shear force of soil. In this case, the shallow surface soil layer turns saturated, and the initial soil water content of following layer is less affected. Infiltration rate declines along with vertical depth direction.

Given the complexity of shallow landslide studies, the following simplifying assumptions are made in the SLIDE model:

(1) The slope is considered infinite with modest soil thickness.
(2) The failure is considered flat and water downflow occurs, both parallel to the slope.
(3) The evapotranspiration, underground seepage and surface flow are avoided in the water balance. Therefore, we assume all rainfall infiltrates into the soil in figure 1. The infiltration amount approximately equals to the maximum of saturated hydraulic conductivity.

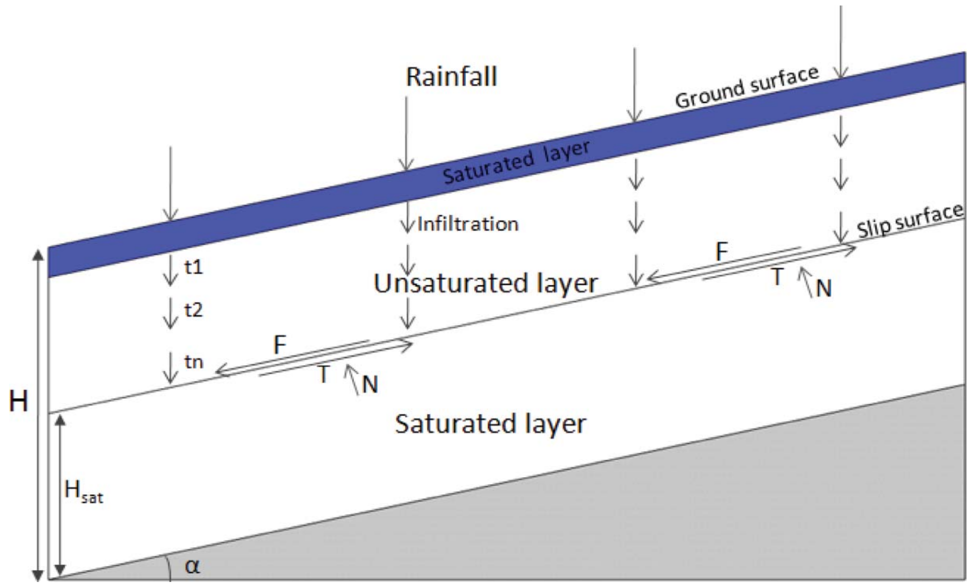

Figure 1. Landslide process from saturated soil infiltration in the SLIDE model.

In this study, we use the infinite-slope equation (Liao et al. 2012) as follows:

$$FS(Z_t, t) = \frac{c' + c(t)}{r_s \cdot Z_t \cdot \sin\alpha \cdot \cos\alpha} + \frac{\tan\phi}{\tan\alpha}, \tag{1}$$

where c' is the soil cohesion, r_s is the unit weight of soil, Z_t is the infiltration depth at time t, and φ is the soil friction angle. $c(t)$ represents the apparent cohesion at time t related to the matric suction, depending on the degree of soil saturation (Montrasio & Valentino 2008), written as

$$c(t) = A \cdot S_r \cdot (1 - S_r)^{\lambda} \cdot (1 - m_t)^{\partial}. \tag{2}$$

In which A is a parameter from soil type that correlates with the peak shear stress at slope failure, S_r is the degree of soil saturation, λ and ∂ are numerical parameters related to the peak of apparent cohesion (Montrasio & Valentino 2008). m_t is a dimensionless value of soil thickness by infiltration, which varies between 0 and 1:

$$m_t = \frac{\sum_{t=1}^{T} I_t}{n \cdot Z_t \cdot (1 - S_r)}, \tag{3}$$

where I_t is the rainfall accumulation at duration time t, n is the porosity. Z_t is calculated by the saturation infiltration process:

$$Z_t = \sqrt{\frac{2 \cdot K_s \cdot H_c \cdot t}{\theta_n - \theta_0}}. \tag{4}$$

In which K_s is the hydraulic conductivity of saturated soil, H_c is the capillary pressure, θ_0 is the initial water content of soil, and θ_n is the water content of saturated soil.

2.2. Data source

The SLIDE model requires multi-source data as follows:

(1) Digital elevation model (DEM) is acquired from the 30-m-resolution ASTER GDEM, which was developed by the Ministry of Economy, Trade and Industry (MET) of Japan and the United States National Aeronautics and Space Administration (NASA) (http://asterweb.jpl.nasa.gov/gdem.asp). Important topographic parameters are derived, including spatial location, elevation and slope angle.
(2) Rainfall intensity data are obtained from the 0.25°-resolution 3B42 V7 products (combining precipitation from multiple satellite and gauge data) every 3 hours of the NASA Tropical Rainfall Measuring Mission (TRMM) Multi-Satellite Precipitation Analysis (TMPA) (http://trmm.gsfc.nasa.gov).
(3) Soil parameter values (the degree of saturation, the unit weight) are acquired from the soil types of Food and Agriculture Organization of the United Nations (FAO; http://www.fao.org/AG/agl/agll/dsmw.htm). Other parameter values (cohesion, porosity, hydraulic conductivity of saturated soil, capillary pressure, friction angle) are confirmed according to 16 soil texture classification (http://ldas.gsfc.nasa.gov/nldas/NLDASsoils.php) and field investigation.
(4) Water content of soil is obtained from retrieval products of surface soil moisture (http://www.falw.vu/~jeur/lprm/). In the studied year, the lowest value in dry season represents the initial water content of soil (θ_0); and the highest value in wet season represents the water content of saturated soil.
(5) Landslide occurring information is collected from 2010, 2011 China Geological Hazards Bulletin (http://www.cigem.gov.cn/).

3. Study hotspots

Most areas with more landslide susceptibility are located in the south of China (Liu et al. 2012). The three study hotspots we select lie in the southwest, southeast, and south central, respectively (figure 2). Based on DEM resolution, the 30 m × 30 m grid represents the hotspot occurring landslide.

The first is located in Dazhai village, Guanling county, the southwestern region of Guizhou province. Lithology consists of dolomite and siltstone from the high to low section of the slope. At 2:00 pm, 28 June 2010, landslides occurred due to continuous heavy rainfall (Point a in figure 2). This accident caused at least 42 deaths and 57 missing, and the detailed description can be found at the link: http://www.chinadaily.com.cn/china/2010-07/04/content_10055801.htm. The second lies in Liutang village, Magui town, the southwestern region of Guangdong province. Proterozoic migmatite makes up its geological structure with high-steep slope, large surface altitude, thin soil layer and poor soil cohesion. Landslides may occur under the action of heavy rainfall. At 9:00 am, 21 September 2010, landslides occurred because of the rainstorm by 'Fanyabi' typhoon (Point b in figure 2) (Tang et al. 2011). It brought at least the deaths of 55 people and left 42 missing, and the detailed description can be found at the link: http://ihrrblog.org/2010/09/23/typhoon-fanapi-more-landslides-and-floods-in-china/. The third is located in Shi Jiadao village, Baqiao district, the provincial capital of Xi'an. The predominant terrain is loess tableland – the underlying soils consisting of loose Malan loess, with many cracks caused by erosion. At 2:10 pm, 17 September 2011, landslides occurred due to persistent heavy rainfall. It caused the deaths of 32 people, and the detailed description can be found at the link: http://www.chinadaily.com.cn/china/2011-09/22/content_13774390.htm (Point c in figure 2).

Figure 3 includes the two-day rainfall accumulation of provincial administrative regions from TMPA 3B42 V7 products and slope angles of the three hotspots. The largest rainfall accumulation nearby achieved 188.72 mm (Guizhou province, 416.16 mm (Guangdong province) and 192.26 mm

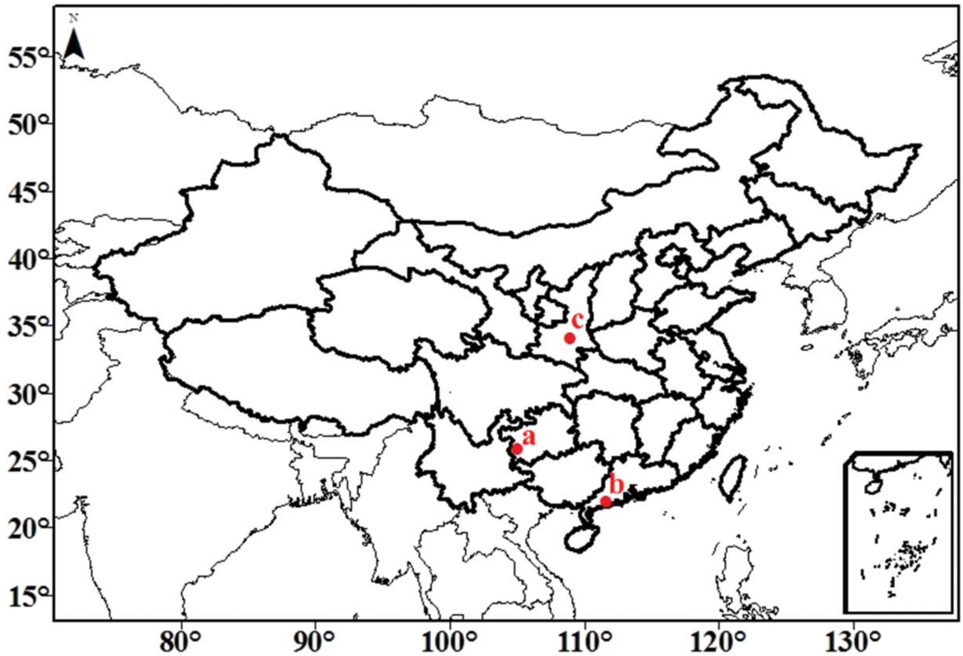

Figure 2. The locations of three hotspots in China.

(Shaanxi province) in landslide occurring, respectively. Meanwhile, the regions prone to landslide have higher slope angle.

4. Results and discussion

4.1. Preliminary analysis on single landslide

The three points in figure 2 represent three study hotpots. Parameter values for the SLIDE model are summarized in table 1. The format of rainfall data (TMPA data) is raster; the other is single number to describe the slope angle, soil information and duration time. As soil parameter values are difficult to assess, we used the general soil textures combined with the *in situ* investigation. In addition, A, λ, and ∂ are theoretically estimated (Montrasio et al. 2009). We combined the above three assumptions with the following two simplifications to implement the SLIDE model.

(1) Vegetation information is ignored in the model because of the fact that the landslide-prone regions have sparse or no vegetation covering (Saha et al. 2005). Accordingly, soil cohesion is only related with soil type in our model.
(2) The soil properties of the layer are considered as homogeneous without preferential flow as model simplified calculation.

With above assumptions, we make the model easily applicable over the three hotspots and able to use various remotely sensed data.

With TMPA data as the rainfall input, FS of three hotspots from the SLIDE model is calculated at 3-hour intervals.

Figure 4 illustrates the relationship between FS of three hotspots and their rainfall. In the first hotspot (figure 4(a)), heavy rainfall was from 9:00 am, 27th June 2010, to 3:00 pm, 28th June

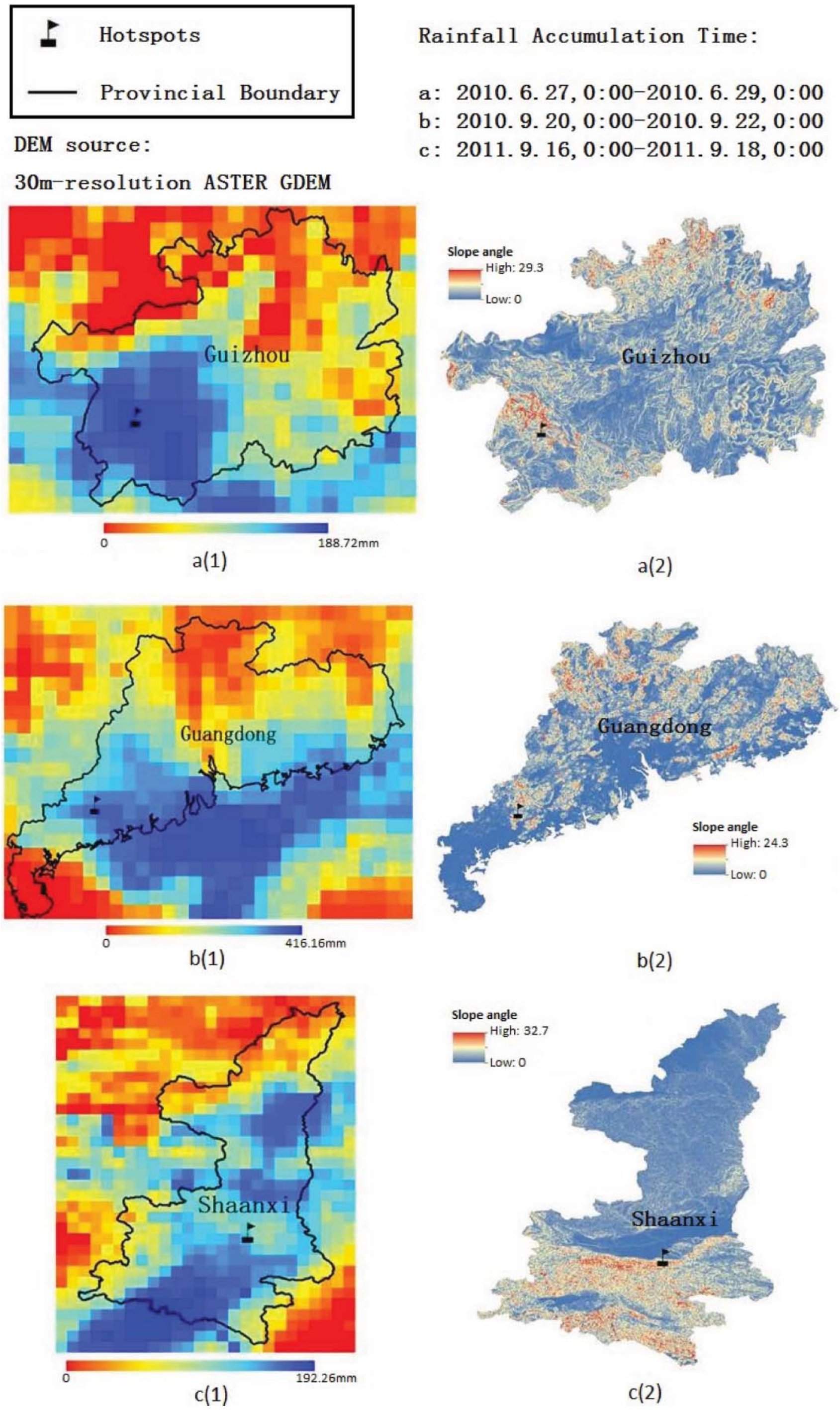

Figure 3. Rainfall accumulation and slope angle in the three hotspots.

2010, for over a 30-hour period. The most significant precipitation (over 140 mm/h) is recorded at 9:00 pm, 27th June 2010.

The SLIDE model shows that unstable (FS $\leq$ 1) time appears before 3:00 pm, 28th June. Actually, landslide occurred at 2:00 pm on 28th June 2010. It is observed that the time calculated by the

Table 1. Parameters used for the SLIDE model.

Parameter			Event ID		
Properties	Symbol	Unit	a	b	c
Location	LAT, LON	Deg	25.94110 N, 105.29569 E	22.21139 N, 111.37089 E	34.28489 N, 109.14075 E
Time	t	s	Varies	Varies	Varies
Rainfall accumulation	I_t	m	Varies	Varies	Varies
Slope angle	a	Deg	30	26	30
Soil type	1−16	Unitless	11	12	14
Parameter shear	A	Unitless	80	100	40
Friction angle	ϕ	Deg	25	22	28
Cohesion	c'	kPa	8	10	13
Coefficient	λ, ∂	Unitless	0.4, 3.4	0.4, 3.4	0.4, 3.4
Unit weight of soil	r_s	k N/m^3	12.5	12.5	13.8
Porosity	n	Unitless	0.40	0.40	0.35
Water content	θ_0, θ_n	Unitless	0.4, 0.9	0.4, 0.9	0.6, 0.9
Degree of saturation	S_r	Unitless	0.19	0.39	0.90
Hydrologic conductivity	K_s	m/s	2.1×10^{-6}	1.8×10^{-5}	1.8×10^{-5}
Capillary	H_c	m	500	500	400

SLIDE model is close to the real time of landslide occurrence. The predicted time from the SLIDE model in the second and third hotspots (figures 4(*b*) and (*c*)) also supports the above observations. The results show that the selected parameters are reasonable and the SLIDE model can simulate rainstorm-induced landslide process.

4.2. Further analysis

From above-mentioned data, we have proved the suitability of the SLIDE model in the rainstorm-induced landslide simulation and evaluation. However, selection of soil parameters is difficult in some regional landslide evaluation because of limited spatial resolution of data involved and spatial heterogeneity of the landslide regions. It is critical to select proper soil parameters for the SLIDE model.

4.2.1. Slope angle variation at slope failure

Combined with formula (2)−(4), formula (1) is transformed as follows:

$$\mathrm{FS}(Z,t) = \frac{t^{-\frac{1}{2}}}{\sin\alpha\ \cos\alpha} \cdot \left[k_1 + k_2 \cdot \left(k_3 \cdot t^{\frac{1}{2}} - \sum_{t=1}^{T} I_t \right)^{\partial} \cdot t^{-\frac{\partial}{2}} + k_4 \cdot t^{\frac{1}{2}} \cdot \cos^2\alpha \right], \tag{5}$$

where k_1, k_2, k_3, and k_4 are parameters of soil information. When soil information is constant, FS is only related to time, slope angle, and rainfall accumulation in formula (5) which is suitable for the top soil saturated condition. When time and rainfall accumulation are acquired, the relationship between slope angle and FS will be calculated. On grounds of news report and SLIDE model results (figure 4), landslide occurred at 29th, 18th and 20th hour after rainstorm began in the three study hotspots, respectively. Because TRMM precipitation products are recorded every 3 hours, we put the duration time (30, 18 and 21 hours) close to landslide occurring time and corresponding rainfall accumulation (211.2, 143.58 and 31.11 mm), to quantify the relationship between FS and slope angle (figure 5).

The red curve in figure 5(*a*), the blue curve in figure 5(*b*) and the green curve in figure 5(*c*) denote the first, second and third hotspots, respectively. The three coincide with the curves that denote the relationship between FS and slope angle. In the three hotpots, landslides may occur ($\mathrm{FS} \leq 1$) in the slope angle between 30° and 85°. As slope angle increases, more of the load force is directed down the slope and steeper slopes are more unstable than shallow slopes without considering other factors.

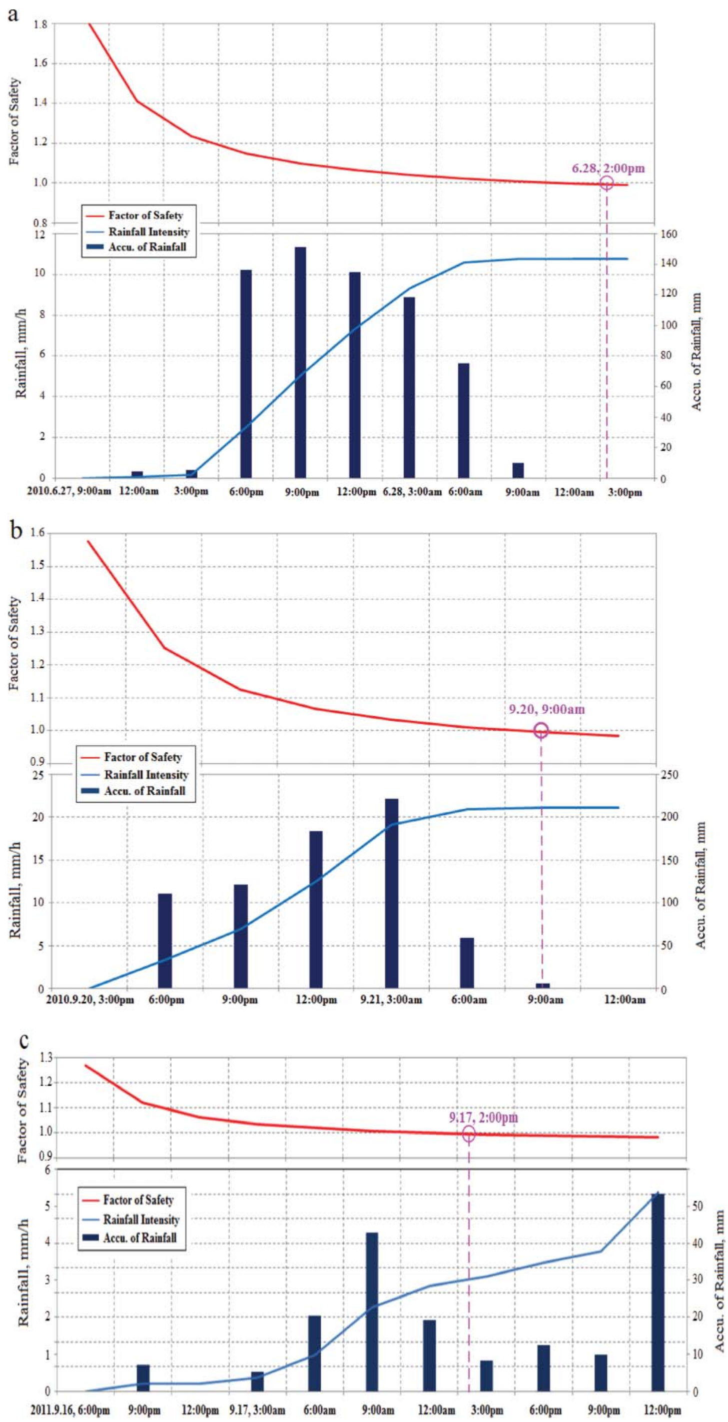

Figure 4. The relationship between FS and rainfall.

At some point, the curves start to decrease, because larger slope angle is that steeper slopes have thicker soil layer and more steady soil textures. This result is consistent with the statistics (most of the landslides occur in the slope angle more than 30°) from the historical landslide records of the past 60 years in China (Liu et al. 2013).

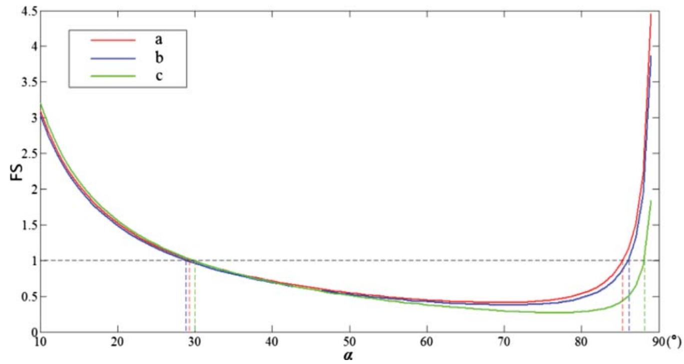

Figure 5. The relationship between FS and slope angle in the three hotspots. (To view this figure in colour, see the online version of the journal.)

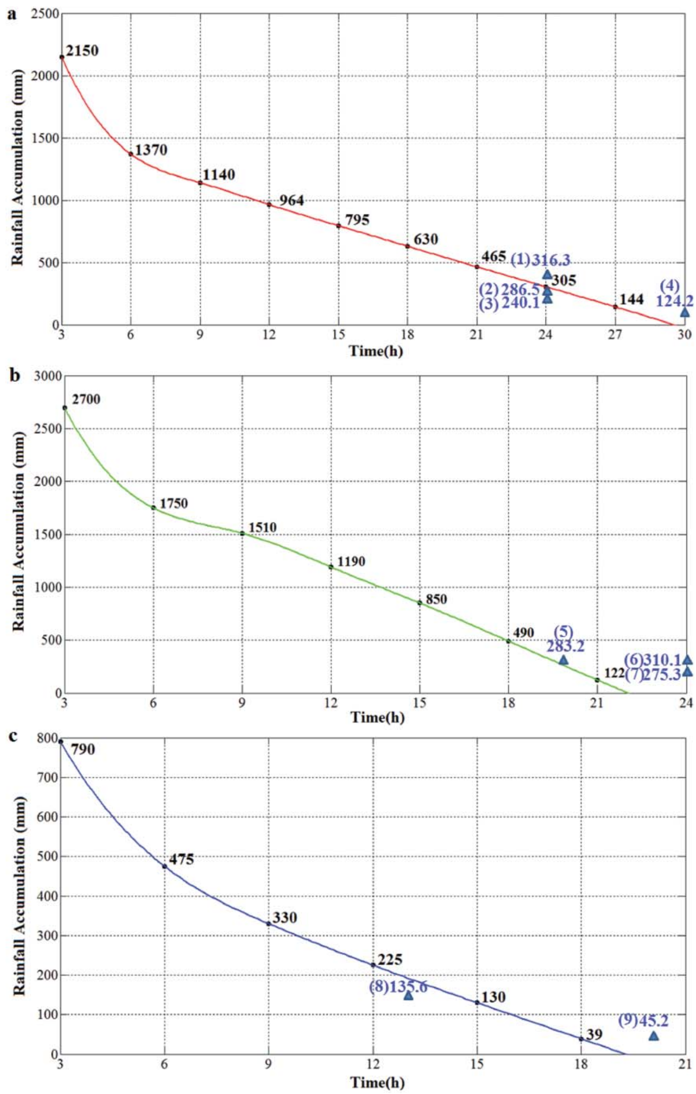

Figure 6. Rainfall accumulation threshold when FS = 1. (To view this figure in colour, see the online version of the journal.)

Table 2. Some landslide records similar with the three hotspots.

ID	Event date	Affected region	Province	Time (h)	Rainfall accumulation (mm)
(1)	6 June 2011	Xintun town	Guizhou	24	316.3
(2)	8 June 2009	Jiarong town	Guizhou	24	286.5
(3)	8 June 2009	Lihua town	Guizhou	24	240.1
(4)	8 June 2009	Rongjiang county	Guizhou	30	124.2
(5)	16 August 2013	Wuhua county	Guangdong	20	283.2
(6)	17 May 2013	Qingyuan	Guangdong	24	310.1
(7)	17 May 2013	Shaoguan	Guangdong	24	275.3
(8)	12 July 2013	Weinan, Xianyang	Shaanxi	13	135.6
(9)	5 July 2011	Lvyang	Shaanxi	20	45.2

4.2.2. Rainfall threshold changes at slope failure

When slope angle and soil information in the equation is static, FS is only related to time and rainfall accumulation in formula (5). Rainfall accumulation varies inversely with time. In the three hotspots (figure 2), slope angle is 30°, 26° and 30°, respectively (table 1). When landslide may occur (FS is close to 1), the relationship between the time and rainfall accumulation can be obtained (figure 6). When soil infiltration satisfies the condition as formula (4) shows in saturated soil layer, the rainfall accumulation (I_t) in landslide occurring varies inversely with time (t). With rainfall time increasing, landslide may occur in lower rainfall accumulation. In other words, the longer the top of soil layer remains saturated, the higher the possibility of landslide occurrence.

In addition, we select the real rainfall accumulation data (table 2) from some other significant landslide records to explain the simulated data. (1), (2), (3), and (4) occurred in Guizhou; (5), (6), and (7) in Guangzhou; (8) and (9) in Shaanxi. The soil textures and slope angles of these regions are same with the three hotspots, respectively. These records are marked in figure 6 as blue triangles. The results show that the threshold of curves are close to the real rainfall accumulation, and prove the SLIDE model to be suitable for rainstorm-induced landslides.

5. Conclusion

A simplified physically based stability forest model SLIDE has been presented for the evaluation of rainstorm-induced landslides in three hotspots in China.

This model integrates the most important impact factors to reveal the landslide occurring. On the basis of three hypotheses in Section 2, the model calculates the FS, taking into account soil and terrain information in saturated soil layers. We selected three typical landslide hotspots located in the southwest, southeast, and south central of China, respectively, and comprehensively testified the model. Results show that the SLIDE model is appropriate for rainstorm-induced landslide simulation: (1) the SLIDE model can simulate the time of rainstorm-induced landslide occurring with reasonable soil parameters; (2) the SLIDE model can quantify the relationship between slope FS, slope angle, and rainfall accumulation with homogenous soil information. The landslides occur (FS $\leq$ 1) in the slope angle more than 30° and relate 24-hour rainfall amount in the three hotspots.

Acknowledgments

The authors thank the editors and reviewers for their suggestions that helped to improve the manuscript.

Disclosure statement

No potential conflict of interest was reported by the authors.

Funding

The work is funded by the National Natural Science Foundation [41501458], [41401389], [41201380]; National Basic Research Program of China [2013CB733204]; Science Program of Shanghai Normal University [SK201525]; Key Laboratory of Mining Spatial Information Technology of NASMG [KLM201309]; Shanghai Gaofeng & Gaoyuan Project for University Academic Program Development; and Center of Spatial Information Science and Sustainable Development Applications, Tongji University, Shanghai, China.

References

Baum RL, Savage WZ, Godt JW. 2008. TRIGRS – a Fortran program for transient rainfall infiltration and grid-based regional slope-stability analysis, version 2. 0. Reston (VA): U.S. Geological Survey.

Beek LPHV, Asch TWJV. 2004. Regional assessment of the effects of land-use change on landslide hazard by means of physically based modelling. Nat Hazards. 31(3):289–304.

Caine N. 1980. The rainfall intensity: duration control of shallow landslides and debris flows. Geogr Annal Series A Phys Geogr. 62:23–27.

Dietrich WE, Montgomery DR. 1998. SHALSTAB: A digital terrain model for mapping shallow landslide potential. Technical Reports. Corvallis (OR): National Council of the Paper Industry for Air and Stream Improvement.

Guzzetti F, Carrara A, Cardinali M, Reichenbach P. 1999. Landslide hazard evaluation: a review of current techniques and their application in a multi-scale study, Central Italy. Geomorphology. 31:181–216.

Heersink P. 2005. World Atlas of natural hazards. Cartographica. 40:133–134.

Hong Y, Adler R, Huffman G. 2007. Use of satellite remote sensing data in the mapping of global landslide susceptibility. Nat Hazards. 43:245–256.

Hong Y, Adler RF. 2008. Predicting global landslide spatiotemporal distribution: integrating landslide susceptibility zoning techniques and real-time satellite rainfall estimates. Int J Sediment Res. 23:249–257.

Huang R, Li W. 2011. Formation, distribution and risk control of landslides in China. J Rock Mech Geotech Eng. 3:97–116.

Iverson RM. 2000. Landslide triggering by rain infiltration. Water Resour Res. 36:1897–1910.

Kirschbaum D, Adler R, Adler D, Peters-Lidard C, Huffman G. 2012a. Global distribution of extreme precipitation and high-Impact landslides in 2010 relative to previous years. J Hydrometeorol. 13:1536–1551.

Kirschbaum DB, Adler R, Hong Y, Kumar S, Peters-Lidard C, Lerner-Lam A. 2012b. Advances in landslide nowcasting: evaluation of a global and regional modeling approach. Environ Earth Sci. 66:1683–1696.

Kuriakose SL, van Beek L, van Westen C. 2008. Comparison of physically based models for debris flow initiation – a case study in the Tikovil river basin of The Western Ghats of Kerala, India. Vienna (Austria): European Geosciences Union General Assembly.

Liao Z, Hong Y, Kirschbaum D, Adler RF, Gourley JJ, Wooten, R. 2011. Evaluation of TRIGRS (transient rainfall infiltration and grid-based regional slope-stability analysis)'s predictive skill for hurricane-triggered landslides: a case study in Macon County, North Carolina. Nat Hazards. 58:325–339.

Liao Z, Hong Y, Kirschbaum D, Liu C. 2012. Assessment of shallow landslides from Hurricane Mitch in central America using a physically based model. Environ Earth Sci. 66:1697–1705.

Liu C, Li WY, Lu P, Sang K, Hong Y, Li RX. 2012. Susceptibility evaluation and mapping of China's landslide disaster based on multi-temporal ground and remote sensing satellite data. Melbourne (Australia):XXII ISPRS Congress.

Liu C, Li W, Wu H, Lu P, Sang K, Sun W, Chen W, Hong Y, Li R. 2013. Susceptibility evaluation and mapping of China's landslides based on multi-source data. Nat Hazards. 69:1477–1495.

Montrasio L, Valentino R. 2008. A model for triggering mechanisms of shallow landslides. Nat Hazard Earth Syst. 8:1149–1159.

Montrasio L, Valentino R, Losi GL. 2009. Rainfall-induced shallow landslides: a model for the triggering mechanism of some case studies in Northern Italy. Landslides. 6:241–251.

Pack R, Tarboton D, Goodwin C. 1998. Terrain stability mapping with SINMAP, technical description and users guide for version 1.00. Terratech Consulting Report. Salmon Arm, BC (Canada): Terratech Consulting.

Petley D. 2012. Global patterns of loss of life from landslides. Geology. 40:927–930.

Saha AK, Arora MK, Gupta RP, Virdi ML, Csaplovics E. 2005. GIS–based route planning in landslide–prone areas. Int J Geogr Inf Sci. 19:1149–1175.

Tang S, Li J, Gu L. 2011. An evaluation model for support capability of railway quick response transportation. Proceedings. Information and Communication Technologies International Symposium (ICTIS) 2011: Multimodal Approach to Sustained Transportation System Development—Information, Technology, Implementation; Wuhan, China; p. 2188–2196.